

Size-effect of fracture parameters for crack propagation in concrete: a comparative study

Shailendra Kumar^{1,2} and S.V. Barai*²

¹Department of Civil Engineering, National Institute of Technology, Jamshedpur-831 014, India

²Department of Civil Engineering, Indian Institute of Technology, Kharagpur-721 302, India

(Received September 1, 2009, Revised February 18, 2011, Accepted April 6, 2011)

Abstract. The size-effect study of various fracture parameters obtained from two parameter fracture model, effective crack model, double- K fracture model and double- G fracture model is presented in the paper. Fictitious crack model (FCM) for three-point bend test geometry for cracked concrete beam of laboratory size range 100-400 mm is developed and the different fracture parameters from size effect model, effective crack model, double- K fracture model and double- G fracture model are evaluated using the input data obtained from FCM. In addition, the fracture parameters of two parameter fracture model are obtained using the mathematical coefficients available in literature. From the study it is concluded that the fracture parameters obtained from various nonlinear fracture models including the double- K and double- G fracture models are influenced by the specimen size. These fracture parameters maintain some definite interrelationship depending upon the specimen size and relative size of initial notch length.

Keywords: concrete fracture; fracture process zone; cohesive stress distribution; nonlinear fracture models; size-effect; three-point bending test.

1. Introduction

During 1960-70s, several experimental and numerical investigations proved that the classical form of linear elastic fracture mechanics (LEFM) approach cannot be applied to normal size concrete members. The inapplicability of LEFM was due to the presence of large and variable size of fracture process zone (FPZ) ahead of the crack-tip. From the past studies it became clear that the fracture mechanics can be a useful and powerful tool for the analysis of growth of distributed cracking and its localization in concrete if the softening behavior of the material is taken into account. The actual application of tension-softening constitutive law was unknown until about mid 1970s. Then using nonlinear fracture mechanics, Hillerborg and co-workers (1976) put forward a pioneer work in which the development of fictitious crack model (FCM) or cohesive crack model (CCM) for the crack propagation study of unreinforced concrete beam was introduced. Thereafter, a number of nonlinear fracture models have been proposed and used to predict the nonlinear fracture behavior of quasibrittle materials like concrete. These are: crack band model (CBM) (Bažant and Oh 1983), two parameter fracture model (TPFM) (Jenq and Shah 1985), size effect model (SEM) (Bažant *et al.* 1986), effective crack model (ECM) (Nallathambi and Karihaloo 1986), K_R -curve method based on cohesive force distribution in the FPZ (Xu and Reinhardt 1998, 1999a), double- K

* Corresponding author, Ph. D., E-mail: skbarai@civil.iitkgp.ernet.in

fracture model (DKFM) (Xu and Reinhardt 1999a,b,c) and double- G fracture model (DGFM) (Xu and Zhang 2008). FCM and CBM are based on the numerical method whereas TPFM, SEM, ECM, K_R -curve method, DKFM and DGFM are based on the modified LEFM concept.

A brief literature survey on the various fracture parameters obtained from different nonlinear fracture models is carried out and presented in the subsequent section. The present contribution will explore the behavior of the different fracture parameters with respect to specimen size and relative size of initial notch length. The main objective of the paper is to show the size-effect behavior of the different fracture parameters obtained using TPFM, SEM, ECM, DKFM and DGFM in a relative manner. The interrelationship of these fracture parameters is also focused and analyzed. For this purpose, FCM for three-point bend test geometry for cracked concrete beam of laboratory size range 100-400 mm is developed and the fracture parameters from SEM, ECM, DKFM and DGFM are evaluated using the required input data obtained from FCM. In addition, similar results of TPFM are obtained with the help of fracture peak load obtained from FCM and the mathematical coefficients reported in the literature (Planas and Elices 1990).

2. Literature review

The cohesive crack model is a simple method and is an idealized approximation of a physical localized fracture zone. The model has great potential to describe the nonlinear material behavior in the vicinity of a crack and at the crack-tip. The non-linearity is automatically introduced by using cohesive stress-crack opening displacement relation (softening function) across the crack faces near the crack-tip, which leads stress intensity factor to be zero. The cohesive crack method was first proposed by Barenblatt (1962) and Dugdale (1960). While Barenblatt (1962) applied cohesive crack method to analyze the brittle fracture behavior, Dugdale (1960) introduced it to model ductile fracture behavior of a material. Hillerborg *et al.* (1976) initially applied cohesive crack method (or fictitious crack model) to simulate the softening damage of concrete structures. Three material properties such as modulus of elasticity E , uniaxial tensile strength f_t , and specific fracture energy G_F are required to describe the cohesive crack model. The G_F is defined as the amount of energy necessary to create one unit of area of a crack. In addition, the shape of softening function of concrete plays an important role on the results predicted by cohesive crack model. RILEM Technical Committee 50-FMC (1985) proposed a method using three point bend test (TPBT) beams to obtain the values of G_F . Although the RILEM recommendation (1985) presented experimental determination of fracture energy using three-point bend test, it has been a matter of discussion in the past because the values of fracture energy obtained from different experiments using RILEM procedure were affected by the specimen size. Planas and co-workers (Guinea *et al.* 1992, Planas *et al.* 1992, Elices *et al.* 1992, 1997) carried out a careful analysis of the test procedure for determination of fracture energy. In the extensive study, Planas and co-workers presented that the apparent size effect on the fracture energy could be reduced by enhancing the experimental method. A detailed explanation for experimental determination of cohesive crack fracture parameters using TPBT such as: tensile strength, initial part of the softening function, fracture energy and bilinear softening curve can be seen in Section 7.3 of the text book (Bažant and Planas 1998). Extensive literature is available on the use of cohesive crack model. The recent studies (Kim *et al.* 2004, Roesler *et al.* 2007, Park *et al.* 2008, Zhao *et al.* 2008, Elices *et al.* 2009) show the applications of cohesive crack model for characterizing the softening functions and predicting the nonlinear fracture characteristics

of concrete using various test configurations.

Bažant and Oh (1983) developed the crack band model in which the fracture process zone is modeled as a system of parallel cracks that are continuously distributed (smeared) in the finite element. The smeared or distributed crack is justified due to presence of random nature of microstructure. The material fracture properties are characterized by three parameters such as: f_t , width of fracture process zone over which the microcracks are assumed to be uniformly spread h_c and G_F (defined as the product of the area under stress-strain curve and h_c). The material behavior is characterized by the constitutive stress-strain relationship.

The two parameter fracture model was developed by Jenq and Shah (1985). In this model, the actual crack is replaced by an equivalent fictitious crack. The model involves two valid fracture parameters for cementitious materials: the critical stress intensity factor K_{IC}^s at the tip of the equivalent crack length at peak load and the corresponding value of the crack-tip opening displacement (CTOD) known as critical crack-tip opening displacement $CTOD_{cs}$. The loading and unloading crack mouth opening displacement (CMOD) compliances of standard three point-bend specimen were used to determine the value of critical effective crack length a_{cs} . RILEM (1990a) procedure is followed for determining the fracture parameters K_{IC}^s and $CTOD_{cs}$ from the test results carried out on the TPBT specimen.

Bažant and co-workers (Bažant *et al.* 1986) introduced size effect model, which describe the material fracture behavior using two parameters: the fracture energy G_f and critical effective crack length extension c_f at peak load for infinitely large test specimen. The fracture parameters are determined from the maximum loads of geometrically similar notched specimen of different sizes according to the RILEM (1990b) guidelines.

Nallathambi and Karihaloo (1986) introduced effective crack model to evaluate effective crack extension Δa_c based on compliance calibration approach. The basic principle of determining the effective crack extension is to obtain the mid-span deflection of the standard three-point-beam test using secant compliance from a typical load-deflection plot up to the peak load P_u and corresponding deflection is δ_u . According to the effective crack model, the fracture in the real structure sets in when the stress intensity factor becomes critical K_{IC}^e at crack length equal to a_e . The details of formulation and calculation procedures of the fracture parameters of effective crack model can be seen in Karihaloo and Nallathambi (1991).

Xu and Reinhardt (1999a) presented the three stages of crack propagation in concrete: crack initiation, stable crack propagation and unstable crack propagation based on tests of the large size compact tension (CT) specimens and small size TPBT specimens. The analysis of these test results advocated double- K fracture model which can represent all the three stages of cracking phenomena in the fracture process of concrete. According to this criterion, the two size independent parameters can be used to describe the fracture process of concrete. The first parameter is termed as initial cracking toughness K_{KC}^{ini} which is directly calculated by the initial cracking load and initial notch length using LEFM formula. The other parameter is known as unstable fracture toughness K_{IC}^{un} which can be obtained by peak load and effective crack length a_c using the same LEFM formula. From the available experimental results, it was also shown that double- K fracture parameters K_{IC}^{ini} and K_{IC}^{un} are not dependent on size of the specimen. Further, the evaluated value of the critical crack-tip opening displacement $CTOD_c$, showed that this value appears to be size dependent (Xu and Reinhardt 1999b). The parameters K_{IC}^{ini} and K_{IC}^{un} computed from fracture tests on the small size wedge-splitting test (WST) specimens shows that these are independent of the relative size of initial notch length, slightly dependent on the size and independent of the thickness of the specimens (Xu and

Reinhardt 1999c).

The K_R -curve method based on cohesive stress distribution in the FPZ introduced by Xu and Reinhardt (1998, 1999a) for complete fracture process description of concrete differs from the conventional method of the R -curve. The distribution of cohesive stress along the FPZ at different stages of loading conditions is taken into account in order to evaluate the K_R -curve which can analyze the complete fracture process of concrete. In addition, the double- K fracture parameters were introduced in the stability analysis using the K_R -curve.

Recently, Xu and Zhang (2008) proposed the double- G fracture criterion based on the concept of energy release rate consisting of two characteristic fracture parameters: the initiation fracture energy release G_{IC}^{ini} and the unstable fracture energy release G_{IC}^{un} . The value of G_{IC}^{ini} is defined as the Griffith fracture surface energy of concrete mix in which the matrix remains still in elastic state under the initial cracking load P_{ini} and the initial crack length a_o . Once the load value P on the structure is increased beyond to the value of P_{ini} , a new crack surface (macro-cracking) is formed and the cohesive stress along the new crack surface starts to act. At the onset of unstable crack propagation, the total energy release G_{IC}^{un} consists of initiation fracture energy release G_{IC}^{ini} and the critical value of the cohesive breaking energy G_{IC}^C . The fracture models based on modified LEFM (TPFM, SEM, ECM, DKFM, K_R -curve associated with cohesive force distribution) are based on stress intensity factor (SIF) concept except for the double- G fracture model which is based on the energy approach. Thereby, the ductility property is also associated with the energy approach based fracture parameters. Extensive test results using two specimen geometries namely TPBT of size range 150-500 mm and WST of size range 200-1000 mm on determination of double- G fracture parameters and double- K fracture parameters were presented by Xu and Zhang (2008). Within certain scatter range in the test results it was concluded that the double- G fracture parameters were size independent over the size range of 200 mm. The double- G fracture parameters were converted to the effective initiation toughness \overline{K}_{IC}^{ini} and effective unstable fracture toughness \overline{K}_{IC}^{un} equivalent to the double- K fracture parameters using the relationship: $K = \sqrt{EG}$. It was found that the values of equivalent fracture parameters in terms of SIF at the onset of crack initiation and the onset of unstable fracture using double- G fracture criterion and double- K fracture criterion are in very close.

It is well known that the nonlinear fracture models capture adequately the structural size-effect

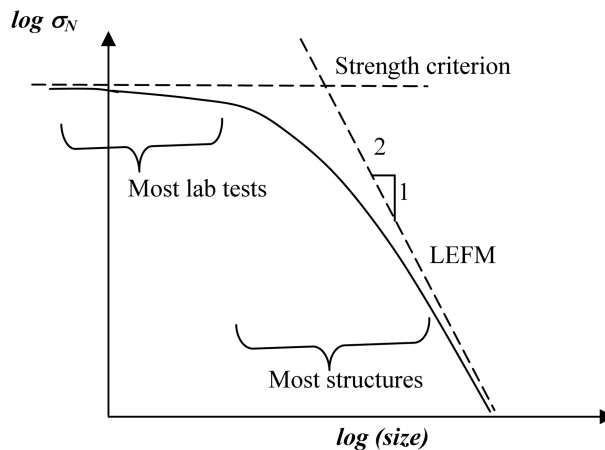


Fig. 1 Size-effects as a plot of nominal strength vs. size on a bilogarithmic scale

over the useful range of applicability. The size-effect is the decrease in nominal strength of geometrically similar structures subjected to symmetrical loads when the characteristic size of the structure is increased. There are two extremes of size-effect law as shown in Fig. 1: (i) strength criteria and (ii) LEFM size-effect. The former yields no size-effect whereas the latter shows the strongest size-effect i.e. nominal strength is inversely proportional to the square root of the structural dimension.

Karihaloo and Nallathambi (1989) used the tests data of three-point bending specimens for the comparison of improved ECM and the TPFM. It was found that predictions from both the models are in good agreement. From the various sources of experimental results, Karihaloo and Nallathambi (1989) showed that fracture toughness values obtained from the ECM and the TPFM and also from the ECM and the SEM are in good agreement. A similar prediction between ECM and TPFM was also observed from the comparison of fracture parameters using different sources of experimental results (Karihaloo and Nallathambi 1991). It was found that irrespective of the concrete strength, the fracture parameters obtained using ECM (K_{IC}^s and a_c) are practically indistinguishable from the corresponding parameters (K_{IC}^s and $CTOD_c$) determined using TPFM.

The size-effect relationships between FCM, SEM and TPFM were developed by Planas and Elices (1990) that predicted almost the same fracture loads for practical size range (100-400 mm) of pre-cracked concrete beam for TPBT geometry. In addition, it was observed from the size-effect study that fracture loads predicted by the SEM and the TPFM could diverge about 28% and 31% respectively for asymptotically large size ($D \rightarrow \infty$) beam. Later, based on the similar approach (Planas and Elices 1990), a size-effect study between FCM and ECM was presented by Karihaloo and Nallathambi (1990). In the study, it was shown that the predicted fracture loads from both the models for the practical size range of TPBT configuration are indistinguishable and in the asymptotic limit (of infinite size), the predictions differed by about 17%.

It was also shown that the numerical results of K_{IC}^s in TPFM and G_f in SEM are very similar (Tang *et al.* 1992, Bažant *et al.* 1991, Bažant 2002) and approximately equivalent throughout the whole size range and the second parameter of each model can be obtained by

$$CTOD_{cs} = \sqrt{\frac{32G_f c_f}{\pi E'}} \quad (1)$$

where E' is $E/(1-\nu^2)$ for plain strain and is E for plain stress case.

Planas and co-workers (Planas and Elices 1990, 1991, 1992, Elices and Planas 1996) carried out extensive studies on size-effect of concrete specimens using various fracture models including CCM, TPFM and SEM. For cohesive crack model, a correlation between fracture energy and the characteristic length as the basic parameters was derived by Planas and Elices (1990, 1991) which depends on the shape of the softening function. Further, the peak load for the cohesive crack model can be completely defined using initial linear softening for the normal experimental range of specimen sizes. An elegant description for correlations of cohesive crack model with Bažant's SEM and Jenq-Shah's TPFM has been presented by Bažant and Planas (1998) in Chapter 7 of their text book. It has been pointed out in the book that a correlation between the fracture parameters of the various models can be established using size effect results. Based on the results of Planas and Elices (1990, 1992), a relationship between cohesive crack fracture energy, tensile strength and horizontal intercept from the initial linear softening for quasi-exponential softening function has presented in the above book. The relation can be further used to determine the cohesive crack characteristic length and the fracture parameters of Bažant's SEM and Jenq-Shah's TPFM. The detailed description and

relationship can be seen in the text book (Bažant and Planas 1998).

Ouyang *et al.* (1996) established an equivalency between TPFM and SEM based on infinitely large size specimens. It was found that the relationship between $CTOD_{cs}$ and c_f theoretically depends on both specimen geometry and initial crack length and both the fracture models can reasonably predict fracture behavior of quasi-brittle materials.

Elices and Planas (1996) also presented a comprehensive review over the relevance to size effect predictions based on comparison of different models of concrete fracture using cohesive crack model as the reference. It was found that simpler models such as: the equivalent elastic crack associated with R -curve approach, Bažant's SEM and Jenq-Shah's TPFM fit inside this scheme and are hierarchically related.

Xu *et al.* (2003) conducted concrete fracture experiments on both the three-point bending notched beams and the wedge splitting specimens with different relative initial crack length according to the experimental requirements for determining the fracture parameters in the double- K fracture model and the two parameter fracture model. The comparative results showed that the critical crack length a_c determined using the two different models are hardly different. The values of K_{IC}^{um} and $CTOD_c$ measured for DKFM are in good agreement with K_{IC}^s and $CTOD_{cs}$ measured for TPFM.

Hanson and Ingraffea (2003) developed the size-effect, two-parameter, and fictitious crack models numerically to predict crack growth in materials for three-point bend test. The investigation showed that if the three models must predict the same response for infinitely large structures, they do not always predict the same response on the laboratory size specimens. However, the three models do agree at the laboratory size specimens for certain ranges of tension softening parameters. It seemed that the relative size of tension softening zone must be less than approximately 15% of the ligament length for the two-parameter fracture model to predict similar behavior as of fictitious crack model. Further, it appeared that the total relative size of tension softening zone is not an indication for the size-effect model to predict the similar response as of the fictitious crack model.

Roesler *et al.* (2007) plotted the size-effect behavior of experimental results, numerical simulation using cohesive crack model, size-effect model and two parameter fracture model for three-point-bend test specimens. From the analysis of results it is found that the size-effect behavior calculated from SEM and TPFM resembles closely.

From the fracture tests (Xu and Zhang 2008), it is also clear that the corresponding values of double- K fracture parameters and double- G fracture parameters are equivalent at initial cracking load and unstable peak load.

Cusatis and Schaffert (2009) presented precise numerical simulations based on cohesive crack model for computation of size-effect curves using typical test configurations. The results were analyzed with reference to SEM to investigate the relationship between the size-effect curves and the size effect law. The practical implications of the study were also discussed in relation to the use of the size-effect curves or the size effect law for identification of the softening law parameters through the size effect method.

Experimental results and analyses available in the literature (Xu and Reinhardt 1999a, 1999b, 1999c) shows that the double- K fracture parameters are almost independent of specimen size. Furthermore, it is pointed that the principles of the development of fictitious crack model and double- K fracture model are contrary to each other. In the development of fictitious crack model, no singularity is considered at the crack-tip whereas, in the double- K fracture model, the cohesive stress does not necessarily abolish the stress singularity condition. To this end, the authors (Kumar and Barai 2010) investigated the size-effect study between FCM and DKFM similar to those for

TPFM, SEM and ECM with reference to FCM. From the study using three-point bend test specimens, it was found that both the fracture models (fictitious crack model and double- K fracture model) yield almost the same values of unstable fracture load and crack initiation load up to 400 mm depth of the beam, beyond this the difference in predicted loads may increase. The predictions in asymptotic behavior of crack initiation load and unstable fracture load with regard to fictitious crack model are relatively varied. These predictions are more conservative by about 20 and 22% respectively for asymptotic large size ($D \rightarrow \infty$). The authors (Kumar and Barai 2008, 2009a) used TPBT and CT specimens of size range $100 \leq D \leq 600$ mm and $100 \leq D \leq 500$ mm respectively to carry out numerical studies on the double- K fracture parameters. In both the studies it was demonstrated that the fracture parameters K_{IC}^{ini} and K_{IC}^{un} are influenced by the specimen size.

The double- G fracture criterion is similar to the double- K fracture model that is the cohesive stress does not necessarily abolish the stress singularity condition unlike to the fictitious crack model. In the numerical study (Kumar and Barai 2009a), the input data obtained from FCM was used to obtain double- G fracture parameters \overline{K}_{IC}^{ini} and \overline{K}_{IC}^{un} it was observed that the parameters are influenced by the specimen size.

From the previous numerical studies carried out by different researchers it is clear that most of the fracture parameters are affected by specimen size. These results have been reported separately and hence it is difficult to make a precise comparison among them. Moreover, a comparative study regarding the other parameters (such as $CTOD_{cs}$ of TPFM, a_e of ECM, a_c and $CTOD_c$ of DKFM or DGFM, c_f of SEM) in each of the fracture model is not focused jointly in the literature. The present paper will address a comparative size-effect study using fracture parameters obtained from TPFM, SEM, ECM, DKFM and DGFM with reference to FCM. Since cohesive crack model is widely used to study the crack propagation phenomenon of concrete, the same model is applied to obtain the input parameters for the other fracture models.

For predicting the crack formation, its propagation and load-CMOD response during fracture and fatigue in concrete, the recent studies can also be referred to. Recently, Gasser (2007) used the discrete crack-concept to study the 3D propagation of tensile-dominated failure in plain concrete. The Partition of Unity Finite Element Method (PUFEM) was applied and the strong discontinuity approach was followed in the numerical modeling. The model was applied to study concrete failure during the PCT3D test and the predicted numerical results were compared to experimental data. The P-CMOD response, the crack formation and the strain field were compared to experimental data of the PCT3D test. The developed numerical concept provides a clear interface for constitutive models and allows an investigation of their impact on complex behavior of concrete cracking under 3D conditions. Phillip (2009) developed a new model using modified energy functionals to account for molecular interactions in the vicinity of crack tips, resulting in Barenblatt cohesive forces, such that the model becomes free of stress singularities. For the consistency of the model, the crack reversibility was allowed and local minimizers of the energy functional were considered. The model was solved in its global as well as in its local version for a simple one-dimensional example. It was concluded that while the global energy minimization has a nonsensical result, predicting failure under any nonzero load, the local minimization correctly predicts failure under a critical positive load. The model also correctly predicts the location of crack formation. Alshoabi (2010) presented the numerical simulation of fatigue crack growth in arbitrary 2D geometries under constant amplitude loading by the using a new finite element software. In the simulation, an automatic adaptive mesh was carried out in the vicinity of the crack front nodes and in the elements which represented the higher stresses distribution. The fatigue crack direction and the corresponding stress-

intensity factors were estimated at each small crack increment by employing the displacement extrapolation technique under facilitation of singular crack tip elements. A consistent transfer algorithm and a crack relaxation method were proposed and implemented in the model. Using several test specimens, the predicted fatigue life was validated with relevant experimental data and numerical results obtained by other researchers. The comparison of the results shows that the developed numerical model is capable of demonstrating the fatigue life prediction results as well as the fatigue crack path satisfactorily.

3. Material properties and determination of fracture parameters

Fictitious crack model or cohesive crack model for standard specimens of three-point bending test as shown in Fig. 2 is developed in the present study.

In this method, the governing equation (Pettersson 1981, Carpinteri 1989) of crack opening displacement (COD) along the potential fracture line is written. Effect of self-weight of the beam is also considered in the numerical model. The influence coefficients of the COD equation are determined using linear elastic finite element method. The COD vector is partitioned according to the enhanced algorithm introduced by Planas and Elices (1991). Finally, the system of nonlinear simultaneous equation is developed and solved using Newton-Raphson method. Several commonly used shapes of softening curves such as bilinear, exponential, nonlinear, quasi-exponential, etc. are available in the literature. The detailed expressions of these softening curves can be found in the literature (Kumar and Barai 2009b). Any of the softening curves like bilinear or nonlinear curve can be considered for the size-effect study however, quasi-exponential softening curve is selected in the present study because some of the parameters of size effect results of TPFM derived by Planas and Elices (1990) have been used in order to obtain fracture parameters for TPFM. The parameters of quasi-exponential function used in the study are: $A = 0.0082896$ and $B = 0.96020$. Same concrete mix (Planas and Elices 1990) is taken in the present investigation for which $f_t = 3.21$ MPa, $E = 30$ GPa, and $G_F = 103$ N/m. The value of ν is assumed to be 0.18. For TPBT specimen of notched concrete beam with $B = 100$ mm, size range $100 \leq D \leq 400$ mm and $S/D = 4$, the finite element analysis is carried out for determining the fracture peak load and the corresponding CMOD using fictitious crack model at initial crack length/depth (a_o/D) ratios ranging between 0.2-0.5. Four noded isoparametric elements are considered for finite element calculation. The half of the beam is

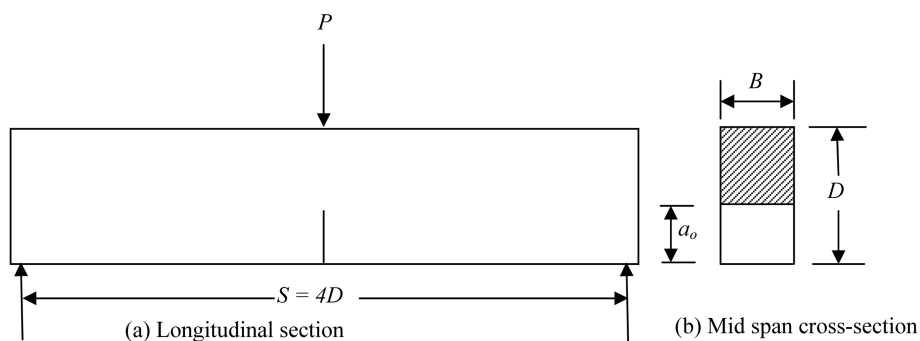


Fig. 2 Three point bending test (TPBT) specimen geometry

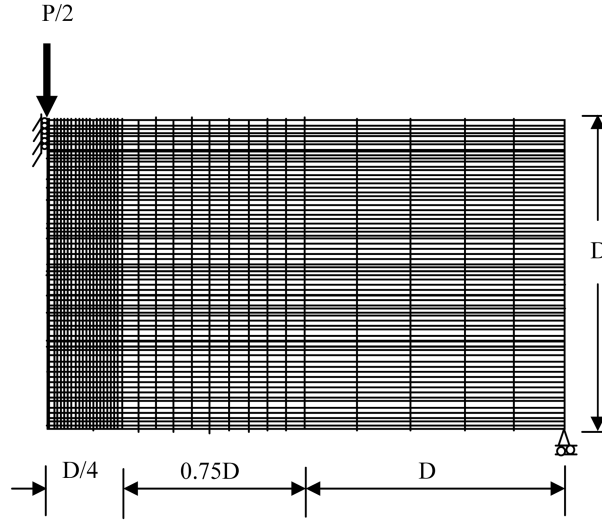


Fig. 3 Finite element discretization of TPBT

Table 1 Peak load and corresponding CMOD for standard TPBT obtained using FCM for material properties: $f'_t = 3.21$ MPa, $E = 30$ GPa and $G_F = 103$ N/m

D (mm)	a_o/D							
	0.2		0.3		0.4		0.5	
	P_u (N)	$CMOD_c$ (μm)						
100	5070.94	32.5	3934.50	41.1	2947.20	48.9	2095.20	58.7
200	8502.80	45.3	6571.40	56.0	4909.70	68.2	3477.20	83.3
300	11276.49	56.1	8672.38	68.8	6447.90	86.8	4529.49	104.5
400	13608.21	62.5	10405.00	79.7	7683.40	99.7	5335.20	118.5

discretized as shown in Fig. 3 and 80 numbers of equal elements are taken along the depth of the beam.

The peak load P_u and corresponding critical value of CMOD ($CMOD_c$) are gained from the numerical model using FCM are presented in Table 1.

The parameter $l_{ch} = EG_F/f'_t{}^2$ of cohesive crack model is used for comparison of numerical results. In addition, the maximum size of coarse aggregate d_{max} is taken as 19 mm for all the subsequent computations. Since loading and unloading during test of fracture specimen is required to obtain the fracture parameters of TPFM: K_{IC}^s and $CTOD_{cs}$ ($CTOD_c$ of TPFM) according to the procedure outlined in RILEM Draft Recommendations TC89-FMT (1990a), it is not possible with the available results obtained using FCM to determine the fracture parameters. Therefore, the parameters K_{IC}^s is precisely evaluated with the help of inverse analysis using the expressions and mathematical coefficients presented by Planas and Elices (1990) in which the authors determined the fracture parameters of TPFM for the same TPBT specimen and material properties. The critical effective crack extension for infinite size $\Delta a_{cs\infty}$ is determined using Eq. (1) in which $c_f = \Delta a_{cs\infty}$, $G_f = G_{FS}$. Finally, the size-effect equation of TPFM is cast in the following form.

$$\frac{EG_{FC}}{K_{INu}^2} = \frac{G_{FC}}{G_{FS}} \left[1 + \frac{\Delta a_{cs\infty}}{l_{ch}} \frac{2k'(\alpha_o)l_{ch}}{k(\alpha_o)D} \right] \quad (2)$$

Where $\alpha = a/D$, $k'(\alpha)$ is the 1st derivative of $k(\alpha)$ with respect to α , G_{FC} is equal G_F and G_{FS} is the equivalent fracture energy obtained using TPFM. In Eq. (2) the mathematical coefficient $\Delta a_{cs\infty}/l_{ch}$ was obtained as 0.0746 (Planas and Elices 1990) for each geometry (a_o/D) ranging between 0.2-0.5 within an accuracy level of 3%. The stress intensity factor K_{IN} corresponding to nominal stress σ_N is determined using LEFM formula given in Tada *et al.* (1985). For three-point-bending test geometry, $S = 4D$, the following formulas are used.

$$K_{IN} = \sigma_N \sqrt{D} k(\alpha) \quad (3)$$

Where $k(\alpha)$ is a geometric factor and σ_N is the nominal stress in the beam due to external load P and self weight of the structure which is given by

$$k(\alpha) = \sqrt{\alpha} \frac{1.99 - \alpha(1 - \alpha)(2.15 - 3.93\alpha + 2.7\alpha^2)}{(1 + 2\alpha)(1 - \alpha)^{3/2}} \quad (4)$$

$$\sigma_N = \frac{3S}{4BD^2} [2P + w_g S] \quad (5)$$

where the w_g is self weight per unit length of the structure. The K_{INu} of Eq. (2) can be obtained using Eq. (3) in which: $K_{IN} = K_{INu}$ for $\sigma_N = \sigma_{Nu}$ (when $P = P_u$) and $\alpha = \alpha_o = a_o/D$. In the present study, the value of K_{INu} is determined using the value of P_u obtained from FCM for a particular TPBT specimen. Then, for a given geometry and material properties, the G_{FS} is determined using Eq. (2). Finally, the $CTOD_{cs}$ is evaluated using Eq. (1) and the K_{IC}^s is calculated using the following LEFM formula.

$$K_{IC}^s = \sqrt{EG_{FS}} \quad (6)$$

The computed values of both the fracture parameters K_{IC}^s and $CTOD_c$ are given in Table 2.

For the given peak load and initial notch length, the fracture parameters of SEM, G_f and c_f are determined adopting the procedure given in RILEM Draft Recommendations TC89-FMT (1990b) for three-point bend test specimen as shown in Fig. 2. Further, the equivalent critical stress intensity factor K_{IC}^b is obtained using the standard LEFM equation for comparison purpose. These results are presented in Table 2.

Fracture parameters K_{IC}^e and a_e of ECM are obtained using the equations given by Karihaloo and Nallathambi (1990). In this method first of all the a_e is obtained by using the regression equation (Karihaloo and Nallathambi 1990) for given material and geometrical properties of a TPBT specimen and then the value of K_{IC}^e is calculated using LEFM equations. Both the fracture parameters determined are presented in Table 2 for TPBT specimen at a_o/D ratios ranging between 0.2-0.5.

The initiation toughness K_{IC}^{in} and unstable fracture toughness K_{IC}^{un} of the TPBT specimen can be obtained using analytical method (Xu and Reinhardt 1999b) in which the numerical integration for determining the cohesion toughness requires specialized numerical technique because of singularity problem at integral boundary. To avoid this difficulty, the authors (Kumar and Barai 2008) put forward application of universal weight function which enables one to calculate the cohesion toughness in a closed form equation without compromising in accuracy of results. Hence, in present study the double- K fracture parameters are determined using five term weight function method as

Table 2 Comparison of various fracture parameters for the material and geometrical properties: $f_t' = 3.21$ MPa, $E = 30$ GPa, $G_F = 103$ N/m, $d_{max} = 19$ mm, $B = 100$ mm, $S/D = 4$

D (mm)	a_e/D	Fracture parameters of SEM		Fracture parameters of TPFM			Fracture parameters of ECM		Double-K fracture parameters				Double-G fracture parameters	
		K_{IC}^b (MPa-m ^{1/2})	c_f (mm)	K_{IC}^s (MPa-m ^{1/2})	$CTOD_{cs}$ (μ m)	$a_{cs\infty}$ (mm)	K_{IC}^e (MPa-m ^{1/2})	a_e/D	K_{IC}^{un} (MPa-m ^{1/2})	K_{IC}^{ini} (MPa-m ^{1/2})	a_e/D	$CTOD_c$ (μ m)	\overline{K}_{IC}^{un} (MPa-m ^{1/2})	\overline{K}_{IC}^{ini} (MPa-m ^{1/2})
100	0.2	1.30	36.73	0.795	12.64	22.4	1.227	0.384	1.224	0.553	0.383	20.24	1.171	0.639
200	0.2			0.934	14.87		1.333	0.346	1.328	0.547	0.345	26.53	1.267	0.637
300	0.2			1.020	16.23		1.431	0.337	1.400	0.532	0.329	31.77	1.335	0.634
400	0.2			1.080	17.19		1.512	0.334	1.419	0.520	0.310	33.76	1.352	0.625
100	0.3	1.31	38.52	0.907	14.43	22.4	1.281	0.485	1.238	0.572	0.474	20.94	1.197	0.659
200	0.3			1.008	16.04		1.334	0.438	1.316	0.565	0.433	26.19	1.267	0.644
300	0.3			1.077	17.14		1.419	0.426	1.377	0.554	0.416	30.68	1.323	0.636
400	0.3			1.128	17.96		1.495	0.423	1.420	0.539	0.405	34.31	1.362	0.626
100	0.4	1.30	36.87	0.973	15.48	22.4	1.357	0.586	1.212	0.576	0.555	20.00	1.177	0.649
200	0.4			1.047	16.66		1.332	0.528	1.299	0.576	0.521	25.49	1.260	0.646
300	0.4			1.103	17.55		1.402	0.515	1.383	0.566	0.510	31.37	1.341	0.647
400	0.4			1.146	18.23		1.473	0.511	1.416	0.553	0.498	34.47	1.372	0.637
100	0.5	1.27	33.91	1.014	16.13	22.4	1.548	0.695	1.188	0.575	0.637	19.05	1.148	0.624
200	0.5			1.065	16.95		1.371	0.626	1.281	0.578	0.609	24.70	1.241	0.627
300	0.5			1.110	17.67		1.416	0.609	1.351	0.572	0.597	29.58	1.310	0.627
400	0.5			1.146	18.23		1.480	0.604	1.370	0.562	0.584	31.59	1.329	0.618

mentioned elsewhere (Kumar and Barai 2008). Since the softening relation of concrete is also required for determining the parameters of DKFM, modified bilinear softening function of concrete (Xu and Reinhardt 1999b, Xu and Zhang 2008) is adopted in present calculation. The effect of self weight on the computation of effective crack length and the fracture parameters are taken into consideration as mentioned by Kumar and Barai (2009a). The results of fracture parameters K_{IC}^{ini} and K_{IC}^{un} for the TPBT specimen are presented in Table 2.

The analytical method (Xu and Zhang 2008, Kumar and Barai 2009a) is used for determining of double- G fracture parameters. Therefore, it is convenient to obtain the effective double- K fracture parameters i.e. effective initiation fracture toughness \overline{K}_{IC}^{ini} and effective unstable fracture toughness \overline{K}_{IC}^{un} in terms of equivalent stress intensity factors using double- G fracture model. Modified bilinear softening function of concrete is also used for determining the fracture parameters of DGFM in present calculation. The computed values of double- G fracture parameters are shown in Table 2. All calculations are performed with developed computer program using MATLAB (Version 7).

4. Size-effect study using various fracture models

4.1 Size-effect of critical stress intensity factors

In Table 2, the K_{IC}^b denotes the equivalent critical value of SIF obtained using G_f and LFM equations. From the table it is clear that the fracture parameters of SEM are independent of specimen size whereas they are marginally dependent on geometrical factor a_o/D ratio. The reason is obvious. In the SEM, the fracture energy G_f by definition is independent of test specimen size although this is true only approximately since the size effect law is not exact. The G_f is also independent of the specimen shape. This becomes clear by realizing that the fracture process zone occupies a negligibly small fraction of the specimen's volume in an infinitely large specimen. Therefore, most of the specimen is elastic, which implies that the fracture process zone at its boundary is exposed to the asymptotic near-tip elastic stress and displacement fields which are known from LFM and are the same for any specimen geometry. Here, the fracture process zone must be in the same state regardless of the specimen shape. For this reason, the computed fracture parameters K_{IC}^s of TPFM, K_{IC}^e of ECM, K_{IC}^{un} and K_{IC}^{ini} of DKFM and \overline{K}_{IC}^{un} and \overline{K}_{IC}^{ini} of DGFM at a_o/D ratios 0.2-0.5 are scaled down to K_{IC}^b and plotted in Figs. 4-7 respectively.

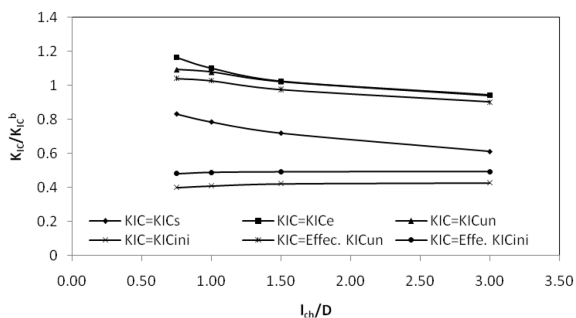


Fig. 4 Size-effect behavior of various fracture parameters at a_o/D ratio = 0.2

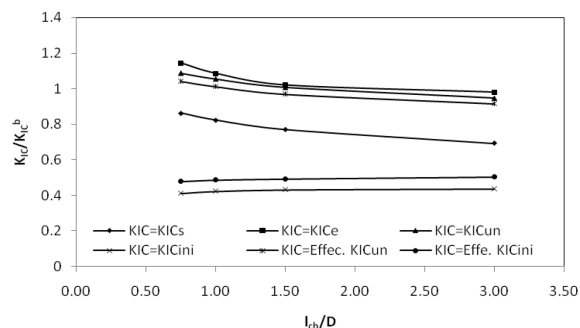


Fig. 5 Size-effect behavior of various fracture parameters at a_o/D ratio = 0.3

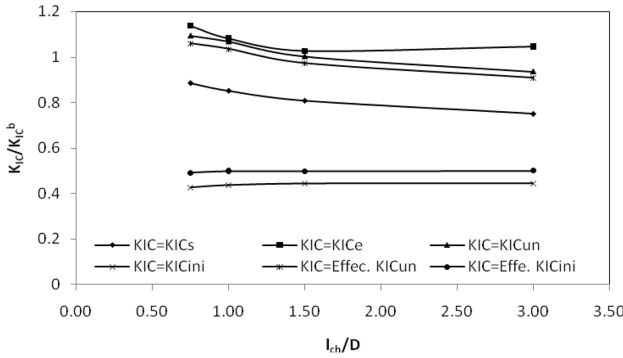


Fig. 6 Size-effect behavior of various fracture parameters at a_o/D ratio = 0.4

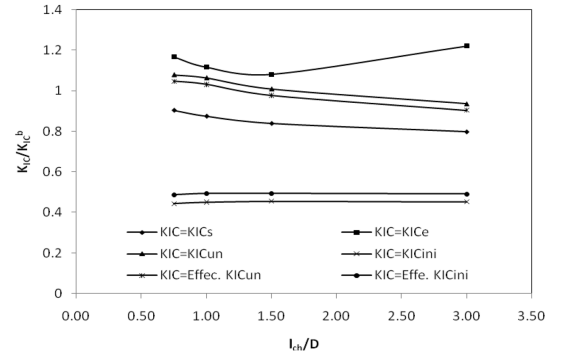


Fig. 7 Size-effect behavior of various fracture parameters at a_o/D ratio = 0.5

From the figures it is observed that all the fracture parameters are influenced by specimen size hence exhibit size-effect. These fracture parameters of various fracture models with reference to K_{IC}^b of SEM maintains certain relationship with the non-dimensional parameter l_{ch}/D . From Fig. 4 it is observed that fracture parameters at critical condition K_{IC}^e of ECM, K_{IC}^{un} of DKFM and $\overline{K_{IC}^{un}}$ of DGFm are close to each other and show similar variation with respect to the l_{ch}/D . Size-effect behavior of K_{IC}^s of TPFM at critical condition is similar to that of the K_{IC}^e , K_{IC}^{un} and $\overline{K_{IC}^{un}}$ however, the magnitude of the K_{IC}^s is somewhat less than those mentioned above. This means that TPFM predicts the most conservative results of critical stress intensity factor at unstable failure. The K_{IC}^{ini} of DKFM and $\overline{K_{IC}^{ini}}$ of DGFm are found to be very close at initial cracking load and show almost similar size-effect behavior.

Figs. 5-7 also show the same size-effect behavior as demonstrated in Fig. 4 except for the parameter of K_{IC}^e of specimen size 100 mm at a_o/D ratio of 0.5. This deviation represented in the figure is due to probably the limitation of the applicability of the regression formula for determining the value of a_e in ECM.

It is observed that the ratio of critical value of stress intensity factors predicted by ECM, DKFM and DGFm to critical value of stress intensity factor predicted by SEM is close to 1. Furthermore, it is evident that the K_{IC}^{ini} and $\overline{K_{IC}^{ini}}$ are less dependent on the specimen size considered in the present study. This behavior was also observed in the previous studies (Kumar and Barai 2008, 2009a). In the numerical study (Kumar and Barai 2008), it was shown that the parameter K_{IC}^{ini} is relatively less dependent on the specimen size ranging between 100-400 mm, however, beyond the size range 400 mm, a decrease in the value is observed. Similarly, the authors (Kumar and Barai 2009a) reported that the parameter K_{IC}^{ini} is almost independent of the specimen size ranging between 100-300 mm and beyond the size range 300 mm, a sharp decrease in the value is observed. In addition, it was observed that the $\overline{K_{IC}^{ini}}$ decreases with the increase in the specimen size. The discrepancy found in the results particularly with the K_{IC}^{ini} and $\overline{K_{IC}^{ini}}$ may be possibly due to different softening functions employed in the calculation because the results of K_{IC}^{ini} and $\overline{K_{IC}^{ini}}$ are somewhat dependent on the softening function of concrete.

From Table 2 and Fig. 4, the ratios of the K_{IC}^s/K_{IC}^b , K_{IC}^e/K_{IC}^b , K_{IC}^{un}/K_{IC}^b , $\overline{K_{IC}^{un}}/K_{IC}^b$, K_{IC}^{ini}/K_{IC}^b and $\overline{K_{IC}^{ini}}/K_{IC}^b$ at a_o/D ratio 0.2 are found to be 0.611, 0.943, 0.941, 0.900, 0.425 and 0.492 respectively for $D = 100$ mm and those are 0.830, 1.162, 1.091, 1.039, 0.400 and 0.481 respectively for $D = 400$ mm. On the other extreme, from Fig. 7, the ratios of the K_{IC}^s/K_{IC}^b , K_{IC}^e/K_{IC}^b , K_{IC}^{un}/K_{IC}^b , $\overline{K_{IC}^{un}}/K_{IC}^b$,

K_{IC}^{ini}/K_{IC}^b and $\overline{K_{IC}^{ini}}/\overline{K_{IC}^b}$ at a_o/D ratio 0.5 are found to be 0.799, 1.220, 0.936, 0.904, 0.453 and 0.492 respectively for $D = 100$ mm and those are 0.903, 1.166, 1.079, 1.047, 0.443 and 0.487 respectively for $D = 400$ mm.

The results indicate that the TPFM predicts the most conservative value of the critical stress intensity factor whereas close results are predicted by the ECM, DKFM and DGFM. The observation is in consistent with the assumptions made for the development of various fracture models. In TPFM, the LEFM equations are applied for computation of different fracture parameters in which only elastic part of the total CMOD is considered for determining the critical effective crack length. The loading and unloading is performed for the measurement of elastic part of the total CMOD. The inelastic part of that CMOD is neglected in calculation which possibly results in relatively lower value of critical effective crack length and K_{IC}^s . In ECM, the nonlinear $P-\delta$ (load-deflection) behavior before attainment of peak load is considered. Similar to compliance calibration method, the peak load and corresponding mid span deflection (secant modulus) is used to evaluate the value of a_e whereas the initial slope of the $P-\delta$ curve is used to determine the elastic modulus of concrete mix. In DKFM or DGFM, the linear superposition assumption (Xu and Reinhardt 1999b) considering P-CMOD plot is used to obtain the critical effective crack length a_c . This assumption can be applied to determine the fictitious effective crack extension for complete analysis of fracture process in concrete. For critical condition, the effective crack length is determined using secant CMOD compliance at peak load whereas the elastic modulus of concrete mix may be determined using initial compliance of P-CMOD plot. Hence, the linear superposition assumption takes into account the nonlinearity effect in the P-CMOD curve before attainment of the unstable condition. This procedure seems to be similar to the method for calculating critical effective crack extension in ECM. From the above explanation it is clear that the K_{IC}^e may be the lowest value whereas the fracture parameters K_{IC}^e , K_{IC}^{un} , $\overline{K_{IC}^{un}}$ should be in close agreement.

4.2 Effect of specimen size on the $CTOD_{cs}$ and $CTOD_c$

The $CTOD_{cs}$ obtained using TPFM and the $CTOD_c$ evaluated using DKFM or DGFM are plotted with respect to the non-dimensional parameter l_{ch}/D in Figs. 8 and 9 respectively.

It is observed from the figures that the $CTOD_{cs}$ and $CTOD_c$ maintain a definite relationship with the specimen size for a given value of a_o/D ratio and they increase as the specimen size increases. It is also observed from the figures that the $CTOD_{cs}$ and $CTOD_c$ depend on the a_o/D ratio for a given

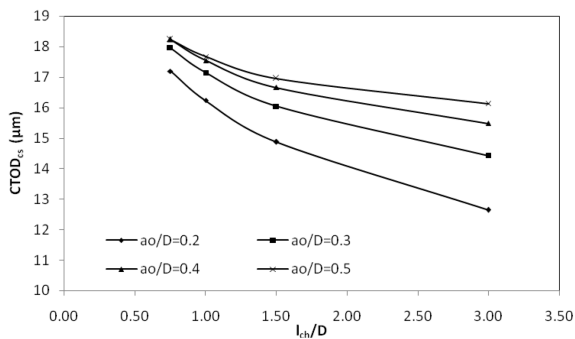


Fig. 8 Size-effect behavior of $CTOD_{cs}$ obtained using TPFM

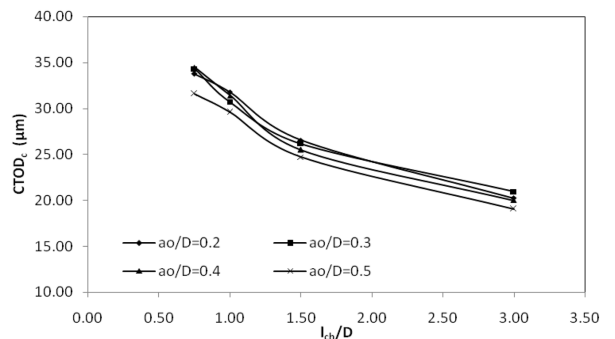


Fig. 9 Size-effect behavior of $CTOD_c$ obtained using DKFM

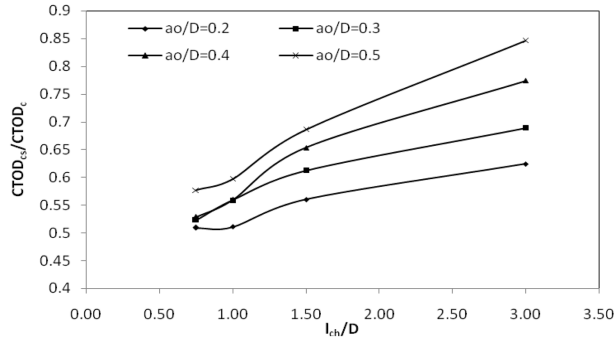


Fig. 10 Relationship of the $CTOD_{cs}$ and $CTOD_c$ obtained between using TPFM and DKFM

specimen size. The values of $CTOD_{cs}$ are more scattered particularly for smaller size of specimens when compared among the different a_o/D ratios whereas those values of $CTOD_c$ are more closer and less scattered and appear to be in a narrow band for size-range 100-400 mm considered in the study.

A relationship between $CTOD_{cs}$ and $CTOD_c$ is presented in Fig. 10 in which the ratio $CTOD_{cs}/CTOD_c$ is plotted with respect to the parameter l_{ch}/D .

It is seen from the figure that the ratio $CTOD_{cs}/CTOD_c$ maintains a definite relationship with the specimen size and the ratio decreases as the specimen size increases. For a_o/D ratio 0.2, the value of $CTOD_{cs}/CTOD_c$ is 0.625, 0.561, 0.511 and 0.509 for specimen size of 100, 200, 300 and 400 mm respectively and the same for a_o/D ratio 0.5 is 0.847, 0.686, 0.597 and 0.577 respectively. Neglecting the effect of a_o/D ratio, the mean values of $CTOD_{cs}/CTOD_c$ for specimen sizes range 100 and 400 mm are determined and found to be 0.734 and 0.535 respectively. It means that the predicted CTOD at critical load using TPFM is relatively more conservative than that predicted by DKFM or DGFM.

4.3 Effect of specimen size on the a_e of ECM and a_c of DKFM or DGFM

The critical effective crack extension ratio a_e/D obtained using ECM and a_c/D computed using DKFM or DGFM are plotted with l_{ch}/D in Figs. 11 and 12 respectively.

A similar trend on both the parameters a_e/D and a_c/D is observed from the figures. The values a_e/D and a_c/D ratios are dependent on a_o/D ratio and specimen size. The assumption for determining both the parameters a_e/D and a_c/D are different. The secant compliance at critical load on P - δ curve

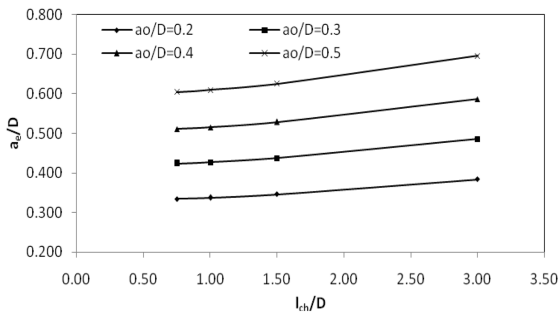


Fig. 11 Size-effect behavior of a_e/D obtained using ECM

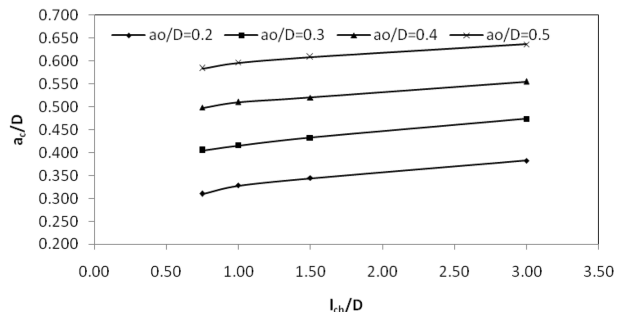


Fig. 12 Size-effect behavior of a_c/D obtained using DKFM

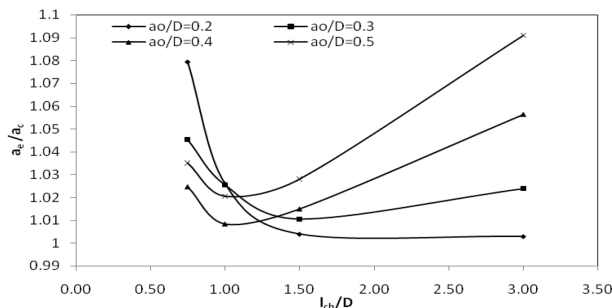


Fig. 13 Relationship of the equivalent critical crack extension obtained between using ECM and DKFM

is used for evaluation of a_e/D ratio whereas the linear superposition assumption is applied on P-CMOD curve to determine the a_o/D value. In present calculation, the regression equation (Karihaloo and Nallathmabi 1990) is used for evaluation of a_o/D ratio while P-CMOD curve with linear superposition assumption is used for determining the a_c/D ratio.

Finally, an interrelation between a_e/D and a_c/D is plotted in Fig. 13.

It is interesting to observe the figure that relationship between a_e/D and a_c/D ratios depends on the specimen size and geometrical factor. However, except for $D = 100$ at $a_o/D = 0.5$, the ratio a_e/a_c is very close to 1 that is effective crack extension at critical load obtained using ECM and DKFM or DGFM is almost equivalent for the size-range considered in the study.

4.4 Relation between c_f of SEM and $a_{cs\infty}$ of TPFM

From Table 2 it is seen that the c_f slightly varies with the a_o/D ratio. For comparison purpose, the mean value of c_f is obtained as 36.51 mm and the mean value of $a_{cs\infty}$ is found as 22.40 mm. The ratio of $a_{cs\infty}/c_f$ is 1.630 which shows that the effective crack extension for infinitely large structures predicted by TPFM is more conservative than the same predicted using SEM by about 38.64%.

5. Conclusions

In the present study the size-effect analysis of various fracture parameters obtained from the important existing fracture models was presented. The fracture parameters were determined on three-point bend test of size-range 100-400 mm for which the input data were obtained from cohesive crack model. A comparative size-effect study was carried out using the possible fracture parameters from TPFM, SEM, ECM, DKFM and DGFM. In general, it was observed that all the fracture parameters were dependent on geometrical factor and specimen size. From present numerical study the following remarks can be highlighted.

- The fracture parameters of all the fracture models including double- K and double- G fracture parameters exhibited size-effect behavior.
- The critical stress intensity factors obtained using SEM, ECM, DKFM and DGFM appear to be close to each other with an error range of $\pm 20\%$.
- TPFM predicted the most conservative critical stress intensity factor.
- The fracture parameters of double- K and double- G fracture models predicted the results very

close to each other at initial cracking and unstable cracking loads.

- The crack-tip opening displacement at unstable fracture load predicted using TPFM was more conservative than that predicted using DKFM or DGFM by about in the range of 27-47%. This value was obtained on the basis of the mean values of crack-tip opening displacement at unstable fracture load from TPFM and DKFM or DGFM for specimen size 100 and 400 mm respectively.
- The critical effective crack length obtained using ECM and DKFM or DGFM was very close to each other.
- The effective crack extension for infinitely large structures predicted by TPFM was more conservative than the same predicted using SEM by about 39%.

References

- Alshoaibi, A.M. (2010), "Finite element procedures for the numerical simulation of fatigue crack propagation under mixed mode loading", *Struct. Eng. Mech.*, **35**(3), 283-299.
- Barenblatt, G.I. (1962), "The mathematical theory of equilibrium cracks in brittle fracture", *Adv. Appl. Mech.*, **7**(1), 55-129.
- Bažant, Z.P. (2002), "Concrete fracture models: testing and practice", *Eng. Fract. Mech.*, **69**, 165-205.
- Bažant, Z.P., Gettu, R. and Kazemi, M.T. (1991), "Identification of nonlinear fracture properties from size effect tests and structural analysis based on geometry-dependent R -curve", *Int. J. Rock Mech. Min.*, **28**(1), 43-51.
- Bažant, Z.P. and Oh, B.H. (1983), "Crack band theory for fracture of concrete", *Mater. Struct.*, **16**(93), 155-177.
- Bažant, Z.P., Kim, J.K. and Pfeiffer, P.A. (1986), "Determination of fracture properties from size effect tests", *J. Struct. Eng. - ASCE*, **112**(2), 289-307.
- Bažant, Z.P. and Planas, J. (1998), *Fracture and size effect in concrete and other quasibrittle materials*, Florida CRC Press.
- Carpinteri, A. (1989), "Cusp catastrophe interpretation of fracture instability", *J. Mech. Phys. Solids*, **37**(5), 567-582.
- Cusatis, G. and Schaufert, E.A. (2009), "Cohesive crack analysis of size effect", *Eng. Fract. Mech.*, **76**, 2163-2173.
- Dugdale, D.S. (1960), "Yielding of steel sheets containing slits", *J. Mech. Phys. Solids*, **8**(2), 100-104.
- Elices, M. and Planas, J. (1996), "Fracture mechanics parameters of concrete an overview", *Adv. Cem. Based Mater.*, **4**, 116-127.
- Elices, M., Guinea, G.V. and Planas, J. (1992), "Measurement of the fracture energy using three-point bend tests: Part 3- Influence of cutting the P - δ tail", *Mater. Struct.*, **25**, 327-334.
- Elices, M., Guinea, G.V. and Planas, J. (1997), "On the measurement of concrete fracture energy using three-point bend tests", *Mater. Struct.*, **30**, 375-376.
- Elices, M., Rocco, C. and Roselló, C. (2009), "Cohesive crack modeling of a simple concrete: experimental and numerical results", *Eng. Fract. Mech.*, **76**, 1398-1410.
- Gasser, T.C. (2007), "Validation of 3D crack propagation in plain concrete. Part II: Computational modeling and predictions of the PCT3D test", *Comput. Concrete*, **4**(1), 67-82.
- Guinea, G.V., Planas, J. and Elices, M. (1992), "Measurement of the fracture energy using three-point bend tests: Part 1 - Influence of experimental procedures", *Mater. Struct.*, **25**, 212-218.
- Hanson, J.H. and Ingraffea, A.R. (2003), "Using numerical simulations to compare the fracture toughness values for concrete from the size-effect, two-parameter and fictitious crack models", *Eng. Fract. Mech.*, **70**, 1015-1027.
- Hillerborg, A., Modeer, M. and Petersson, P.E. (1976), "Analysis of crack formation and crack growth in concrete by means of fracture mechanics and finite elements", *Cement Concrete Res.*, **6**, 773-782.
- Jenq, Y.S. and Shah, S.P. (1985), "Two parameter fracture model for concrete", *J. Eng. Mech. - ASCE*, **111**(10), 1227-1241.

- Karihaloo, B.L. and Nallathambi, P. (1989), "An improved effective crack model for the determination of fracture toughness of concrete", *Cement Concrete Res.*, **19**, 603-610.
- Karihaloo, B.L. and Nallathambi, P. (1990), "Size-effect prediction from effective crack model for plain concrete", *Mater. Struct.*, **23**(3), 178-185.
- Karihaloo, B.L. and Nallathambi, P. (1991), "Notched beam test: mode I fracture toughness", Fracture Mechanics Test methods for concrete, Report of RILEM Technical Committee 89-FMT (Edited by S.P. Shah and A. Carpinteri), Chamman & Hall, London, 1-86.
- Kim, J.K., Lee, Y. and Yi, S.T. (2004), "Fracture characteristics of concrete at early ages", *Cement Concrete Res.*, **34**, 507-519.
- Kumar, S. and Barai, S.V. (2008), "Influence of specimen geometry and size-effect on the K_R -curve based on the cohesive stress in concrete", *Int. J. Fracture*, **152**, 127-148.
- Kumar, S. and Barai, S.V. (2009a), "Equivalence between stress intensity factor and energy approach based fracture parameters of concrete", *Eng. Fract. Mech.*, **76**, 1357-1372.
- Kumar, S. and Barai, S.V. (2009b), "Effect of softening function on the cohesive crack fracture parameters of concrete CT specimen", *Sadhana-Acad. P. Eng. S.*, **36**(6), 987-1015.
- Kumar, S. and Barai, S.V. (2010), "Size-effect prediction from the double- K fracture model for notched concrete beam", *Int. J. Damage Mech.*, **9**, 473-497.
- Kwon, S.H., Zhao, Z. and Shah, S.P. (2008), "Effect of specimen size on fracture energy and softening curve of concrete: Part II. Inverse analysis and softening curve", *Cement Concrete Res.*, **38**, 1061-1069.
- MATLAB, Version 7, The MathWorks, Inc., Copyright 1984-2004.
- Nallathambi, P. and Karihaloo, B.L. (1986), "Determination of specimen-size independent fracture toughness of plain concrete", *Mag. Concrete Res.*, **38**(135), 67-76.
- Ouyang, C., Tang, T. and Shah, S.P. (1996), "Relationship between fracture parameters from two parameter fracture model and from size effect model", *Mater. Struct.*, **29**(2), 79-86.
- Park, K., Paulino, G.H. and Roesler, J.R. (2008), "Determination of the kink point in the bilinear softening model for concrete", *Eng. Fract. Mech.*, **7**, 3806-3818.
- Petersson, P.E. (1981), "Crack growth and development of fracture zone in plain concrete and similar materials", Report No. TVBM-100, Lund Institute of Technology.
- Philip, P. (2009), "A quasistatic crack propagation model allowing for cohesive forces and crack reversibility", *Interact. Multiscale Mech.*, **2**(1), 31-44.
- Planas, J. and Elices, M. (1990), "Fracture criteria for concrete: mathematical validations and experimental validation", *Eng. Fract. Mech.*, **35**, 87-94.
- Planas, J. and Elices, M. (1991), "Nonlinear fracture of cohesive material", *Int. J. Fracture*, **51**, 139-157.
- Planas, J. and Elices, M. (1992), "Shrinkage eigenstresses and structural size-effects", *In Fracture Mechanics of Concrete Structures*, Z.P. Bazant, ed., Elsevier Applied Science, London, 939-950.
- Planas, J., Elices, M. and Guinea, G.V. (1992), "Measurement of the fracture energy using three-point bend tests: Part 2-Influence of bulk energy dissipation", *Mater. Struct.*, **25**, 305-312.
- RILEM Draft Recommendation (TC50-FMC) (1985), "Determination of fracture energy of mortar and concrete by means of three-point bend test on notched beams", *Mater. Struct.*, **18**(4), 287-290.
- RILEM Draft Recommendations (TC89-FMT) (1990a), "Determination of fracture parameters (K_{IC}^c and $CTOD_c$) of plain concrete using three-point bend tests", *Mater. Struct.*, **23**(138), 457-460.
- RILEM Draft Recommendations (TC89-FMT) (1990b), "Size-effect method for determining fracture energy and process zone size of concrete", *Mater. Struct.*, **23**(138), 461-465.
- Roesler, J., Paulino, G.H., Park, K. and Gaedicke, C. (2007), "Concrete fracture prediction using bilinear softening", *Cement Concrete Compos.*, **29**, 300-312.
- Tada, H., Paris, P.C. and Irwin, G. (1985), *The stress analysis of cracks handbook*, Paris Productions Incorporated, St. Louis, Missouri, USA.
- Tang, T., Shah, S.P. and Ouyang, C. (1992), "Fracture mechanics and size effect of concrete in tension", *J. Struct. Eng. - ASCE*, **118**(11), 3169-3185.
- Xu, S. and Reinhardt, H.W. (1998), "Crack extension resistance and fracture properties of quasi-brittle materials like concrete based on the complete process of fracture", *Int. J. Fracture*, **92**, 71-99.
- Xu, S. and Reinhardt, H.W. (1999a), "Determination of double- K criterion for crack propagation in quasi-brittle

- materials, Part I: Experimental investigation of crack propagation”, *Int. J. Fracture*, **98**,111-149.
- Xu, S. and Reinhardt, H.W. (1999b), “Determination of double- K criterion for crack propagation in quasi-brittle materials, Part II: Analytical evaluating and practical measuring methods for three-point bending notched beams”, *Int. J. Fracture*, **98**, 151-77.
- Xu, S. and Reinhardt, H.W. (1999c), “Determination of double- K criterion for crack propagation in quasi-brittle materials, Part III: compact tension specimens and wedge splitting specimens”, *Int. J. Fracture*, **98**, 179-193.
- Xu, S. and Zhang, X. (2008), “Determination of fracture parameters for crack propagation in concrete using an energy approach”, *Eng. Frac. Mech.*, **75**, 4292-4308.
- Xu, S., Reinhardt, H.W., Wu, Z. and Zhao, Y. (2003), “Comparison between the double- K fracture model and the two parameter fracture model”, *Otto-Graf J.*, **14**, 131-158.
- Zhao, Z., Kwon, S.H. and Shah, S.P. (2008), “Effect of specimen size on fracture energy and softening curve of concrete: Part I. Experiments and fracture energy”, *Cement Concrete Res.*, **38**, 1049-1060.

CC

Abbreviations

CBM	crack band model
CCM	cohesive crack model
CMOD	crack mouth opening displacement
CMOD _c	critical value of crack mouth opening displacement
COD	crack opening displacement
CT	compact tension
CTOD	crack-tip opening displacement
CTOD _c	critical value of crack-tip opening displacement
DGFM	double- G fracture model
DKFM	double- K fracture model
ECM	effective crack model
FCM	fictitious crack model
FPZ	fracture process zone
LEFM	linear elastic fracture mechanics
SEM	size effect model
SIF	stress intensity factor
TPBT	three-point bending test
TPFM	two parameter fracture model
WST	wedge-splitting test